CHEMISTRY OF MATERIALS
Communication

*Chem. Mater.* **2009,** *21,* 5007–5009 5007
DOI:10.1021/cm902524h

# $AgCrS_2$: A Spin Driven Ferroelectric

K. Singh, A. Maignan,* C. Martin, and Ch. Simon

*Laboratoire CRISMAT, UMR 6508 CNRS/ENSICAEN, 6 bd du Maréchal Juin, F-14050 CAEN Cedex 4, France*

*Received August 17, 2009*
*Revised Manuscript Received September 29, 2009*

In these last years, intensive research has been devoted to multiferroic materials. Among them, the most interesting candidates for applications are those in which there exists a coupling between the ferroic properties. From a practical viewpoint, this would be appealing to switch the magnetization (or electric polarization) of magnetic (ferroelectric) memories under the application of an electrical (magnetic) field. The realization of such a coupling between ordered spins (ferro- or antiferromagnetism) and electric polarization (ferroelectricity) is a very puzzling problem: the off-centering of the cations responsible for the electric dipoles is generally exclusive with magnetic ordering as $d^0$ or $d^{10}$ cations are involved.[1,2] Nonetheless, there exists exceptions such as the magnetoelectric coupling in $BiFeO_3$, for which the coexistence of magnetism ($Fe^{3+}$) and ferroelectricity ($6s^2$ lone pair of $Bi^{3+}$) comes from different crystallographic sites (Fe and Bi lying at the B octahedra centers and A cages, respectively, of the $ABO_3$ perovskite)[3] or composites and artificial heterostructures in which the coupling results from the interfacial regions between the ferroelectric and (anti)ferromagnetic regions.[4] Remarkably, several magnetic transition metal oxides with broken space-inversion symmetry have been recently shown to provide a new class of magnetoelectrics by going beyond the classical symmetry group theory of ferroelectrics.[5−10] For these so-called "spin driven ferroelectrics", it is the noncollinear spin spiral structure which is responsible for the inversion symmetry breaking. On the one hand, from the experimental side, the members of this oxides subclass are numerous: $TbMnO_3$,[5] $TbMn_2O_5$,[6] $Ba_{0.5}Sr_{1.5}Zn_2Fe_{12}O_{22}$,[7] $Ni_3V_2O_8$,[8] $CoCr_2O_4$,[9] $MnWO_4$,[10] $CuFe_{1-x}M_xO_2$,[11−17] and $ACrO_2$,[18,19] with some compounds with polarization observed at temperatures approaching room temperature such as CuO [20] and $YBaCuFeO_5$.[21] On the other hand, the microscopic origin of the spin driven ferroelectricity is still a matter of debate. The spin current [22,23] and other models,[24−26] which for several compounds are successful to explain the magnetoelectric coupling, have been recently challenged by the reports on spin driven ferroelectricity for $RbFe(MoO_4)_2$ [27] and for delafossites such as $CuFeO_2$,[11,12] $CuFe_{1-x}M_xO_2$ (M = Al, Ga, Rh) [13−17] and $ACrO_2$.[18,19] One common feature of all the latter is their triangular antiferromagnetic planes responsible for an in-plane polarization which cannot be explained by the aforementioned models. The proposed alternative models are in fact based on the existence of ligand−metal orbital hybridization associated to spin−orbit coupling.[28]

Keeping this in mind and considering that in most of the spin driven ferroelectrics the ligands are oxygen anions, it is important to test isostructural compounds with a similar cation framework but different ligands. In that respect, the layer chalcogenides of $MCrX_2$ general composition (M = Ag, Cu, Na, Li; X = S, Se)[29−34] are of

(1) Hill, N. A. *J. Magn. Magn. Mater*. **2002**, *242*, 976.
(2) Khomskii, D. I. *J. Magn. Magn Mater*. **2006**, *306*, 1.
(3) Lebeugle, D.; Colson, D.; Forget, A.; Viret, M.; Bataille, A. M.; Gukasov, A. *Phys. Rev. Lett*. **2008**, *100*, 227602.
(4) For a review see for instance *Magnetoelectric interaction phenomena in crystals*; Fiebig, M., Eremenko, V. V., Chupis, I. E., Eds.; Nato Science Series; Kluwer Academic Publishers: Dordrecht, 2004.
(5) Kimura, T.; Goto, T.; Shintani, H.; Ishizaka, K.; Arima, T.; Tokura, Y. *Nature* (*London*) **2003**, *426*, 55.
(6) Hur, N.; Park, S.; Sharma, P. A.; Ahn, J. S.; Guha, S.; Cheong, S. W. *Nature* **2004**, *429*, 392.
(7) Kimura, K.; Lawes, G.; Ramirez, A. P. *Phys. Rev. Lett*. **2005**, *94*, 137201.
(8) Lawes, G.; Harris, A. B.; Kimura, T.; Rogado, N.; Cava, R. J.; Aharony, A.; Entin-Wohlman, O.; Yildrim, T.; Kenzelmann, M.; Broholm, C.; Ramirez, A. P. *Phys. Rev. Lett*. **2005**, *95*, 087205.
(9) Yamasaki, Y.; Myasaka, S.; Kaneko, Y.; He, J. P.; Arima, T.; Tokura, Y. *Phys. Rev. Lett*. **2006**, *96*, 207204.
(10) Taniguchi, K.; Abe, N.; Takenobu, T.; Iwasa, Y.; Arima, T. *Phys. Rev. Lett*. **2006**, *97*, 097203.
(11) Ye, F.; Ren, Y.; Huang, Q.; Fernandez-Bacan, J. A.; Dai, P.; Lynn, J. W.; Kimura, T. *Phys. Rev. B* **2006**, *73*, 220404.
(12) Kimura, T.; Lashley, J. C.; Ramirez, A. P. *Phys. Rev. B* **2006**, *73*, 220401(R).
(13) Kanetsuki, S.; Mitsuda, S.; Nakajima, T.; Anazawa, D.; Katori, H. A.; Prokes, K. *J. Phys.: Condens. Matter* **2007**, *19*, 145244.
(14) Seki, Y.; Yamasaki, Y.; Shiomi, S.; Iguchi, Y.; Onose; Tokura, Y. *Phys. Rev. B* **2007**, *75*, 100403(R).
(15) Nakajima, T.; Mitsuda, S.; Kanetsuki, S.; Tanaka, K.; Fujii, K.; Terada, N.; Soda, M.; Matsuura, M.; Hirota, K. *Phys. Rev. B* **2008**, *77*, 052401.
(16) Terada, N.; Nakajima, T.; Mitsuda, S.; Kitazawa, H.; Kaneko, K.; Metoki, N. *Phys. Rev. B* **2008**, *78*, 014101.
(17) Kundys, B.; Maignan, A.; Pelloquin, D.; Simon, Ch. *Solid State Sci*. **2009**, *11*, 1035.
(18) Seki, S.; Onose, Y.; Tokura, Y. *Phys. Rev. Lett*. **2008**, *101*, 067204.
(19) Kimura, K.; Nakamura, H.; Ohgushi, K.; Kimura, T. *Phys. Rev. B* **2008**, *78*, 140401.
(20) Kimura, T.; Seiko, Y.; Nakamura, H.; Siegrest, T.; Ramirez, A. P. *Nat. Mater*. **2008**, *7*, 291.
(21) Kundys, B.; Maignan, A.; Simon, Ch. *Appl. Phys. Lett*. **2009**, *94*, 072506.
(22) Katsura, H.; Nagasoa, N.; Balatsky, A. V. *Phys. Rev. Lett*. **2005**, *95*, 057205.
(23) Mostovoy, M. *Phys. Rev. Lett*. **2006**, *96*, 067601.
(24) Arima, T.; Tokunga, A.; Goto, T.; Kimura, K.; Noda, Y.; Tokura, Y. *Phys. Rev. Lett*. **2006**, *96*, 097202.
(25) Sergienko, I. A.; Sen, C.; Dagotto, E. *Phys. Rev. Lett*. **2006**, *97*, 227204.
(26) Chapon, L. C.; Radaelli, P. G.; Blake, G. R.; Park, S.; Cheong, S. W. *Phys. Rev. Lett*. **2006**, *96*, 097601.
(27) Kenzelmann, M.; Lawes, G.; Harris, A. B.; Gasparovic, G.; Broholm, C.; Ramirez, A. P.; Jorge, G. A.; Jaime, M.; Park, S.; Huang, Q.; Ya, A.; Shapiro; Demianets, L. A. *Phys. Rev. Lett*. **2007**, *98*, 267205.
(28) Arima, T. *J. Phys. Soc. Jpn*. **2007**, *76*, 073702.
(29) Bongers, P. F.; Van Bruggen, C. F.; Koopstra, J.; Omloo, W. P. F. A. M.; Wiegers, G. A.; Jellinek, F. *J. Phys. Chem. Solids* **1968**, *29*, 977.
(30) Engelsman, F. M. R.; Van Laar, B.; Weegers, G. A.; Jellinek, F. *Acta Crystallogr., Sect. A* **1969**, *25*, S 247.

© 2009 American Chemical Society
Published on Web 10/09/2009

interest as their $CrX_2$ layers are similar to that of the $MCrO_2$ delafossite and as they order antiferromagnetically with $T_N$ values (19−50 K) not far from that of $CuCrO_2$ ($T_N$ = 24 K) or $AgCrO_2$ ($T_N$ = 21 K).[18] In this Communication, we report on the characterizations of the chromium disulfides, $AgCrS_2$ and $CuCrS_2$. The former, known for its superionic conductivity at high temperature,[35] is also an insulating antiferromagnet ($T_N$ = 42 K),[34] whereas the electronic conduction of the latter does not allow dielectric measurements to be performed. Interestingly, the magnetic ordering of $AgCrS_2$ is found to induce a polarization of similar magnitude to that of $AgCrO_2$.[18] The evidence for spin driven ferroelectricity in this sulphide confirms the important role of the triangular antiferromagnets to generate magnetoelectrics.

The preparation of the polycrystalline sample of $AgCrS_2$ and $CuCrS_2$ together with characterizations (including dielectric and polarization measurements) are given in the Supporting Information.

In agreement with previous reports,[29,31,36] the structural refinements of X-ray powder diffraction data (collected at RT with Cu Kα radiations) have been performed, by using the Fullprof software,[37] in the acentric *R*3*m* rhombohedral space group (hexagonal setting). The results are summarized in Figure 1 for $AgCrS_2$ with a drawing of the structure. It can be described by a stacking of layers of edge-sharing $CrS_6$ distorted octahedra and $AgS_4$ tetrahedra along the *c*-axis. In fact, rather than the octahedral coordination found in the delafossite structure, the trivalent Cr cation adopts a trigonal prismatic coordination [29] with two sets of three Cr−S interatomic distances (about 2.386 Å and 2.447 Å). Similarly, the $Ag^+$ tetrahedral coordination is not regular with one short and three long Ag−S distances. Although the in-plane interatomic distances, Cr−Cr, Ag−Ag, $S_1$−$S_1$, and $S_2$−$S_2$, are equivalent along the different directions of the triangular lattice, the Cr−Ag distances along *c* are asymmetric (3.202 Å and 4.162 Å).

As illustrated by the *T*-dependent magnetic susceptibility ($\chi$) and corresponding reciprocal magnetic susceptibility curves (Figure 2), the magnetic properties of $AgCrS_2$ and $CuCrS_2$ are very similar, with $T_N$ = 42 K and 39 K for $AgCrS_2$ and $CuCrS_2$, respectively. The effective paramagnetic moments deduced from the Curie−Weiss fitting of the linear part of the $\chi^{-1}(T)$ curves in the 100 K−400 K temperature range, $\mu_{eff} = 3.58\,\mu_B$ and $3.46\,\mu_B$ for $AgCrS_2$ and $CuCrS_2$, respectively, and the $T_N$ values, all in good consistency with previous works,[29−34] are larger than those reported for the corresponding $ACrO_2$ oxides, $T_N$ values being 21 K and 24 K for A = Ag and Cu, respectively.

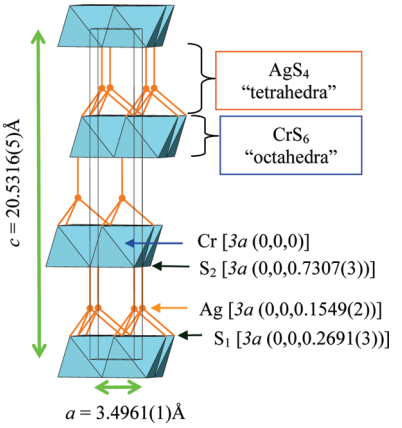


**Figure 1.** Drawing of the structure, showing the layers stacked along the *c*-axis.

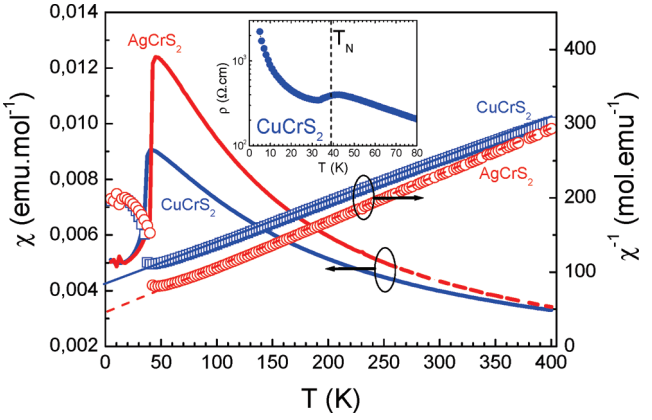


**Figure 2.** Comparison of the $\chi(T)$ curves of $AgCrS_2$ and $CuCrS_2$ showing the slightly higher $T_N$ of $AgCrS_2$ ($T_N$ = 42 K) than that of $CuCrS_2$ ($T_N$ = 39 K). The $\chi^{-1}(T)$ experimental curves (squares) and corresponding linear Curie−Weiss fits (straight lines) are also given (right *y*-axis). Inset: *T*-dependent electrical resistivity $\rho$ of $CuCrS_2$ measured by the four-probe technique. These values are much smaller than those collected for $CuCrO_2$, which increase beyond $10^5$ Ω·cm as *T* becomes lower than 200 K and still reaches $10^3$ Ω·cm at 300 K. For $CuCrS_2$ a clear change of the $\rho(T)$ slope is seen at $T_N \sim 42$ K implying charge/spin coupling. The $\chi$ data are collected within 0.1 T after a zero-field-cooling.

The comparison of the electrical resistivity ($\rho$) shows a major difference between sulfides and oxides. The $\rho$ values are measurable over all *T* values with $\rho_{300K}$ = 20 Ω·cm (Figure 2, inset) for $CuCrS_2$ whereas they are beyond $10^5$ Ω·cm below *T* = 200 K with $\rho_{300K} = 10^3$ Ω·cm for $CuCrO_2$.[38] For the former, $\rho(T)$ measurements allow an anomaly at $T_N$ to be revealed (inset of Figure 2) suggesting the existence of strong spin/charge coupling in the sulfides as in the oxides. Contrasting with the $CuCrS_2$ behavior, excluding dielectric measurements to be made, $AgCrS_2$ exhibits a much more insulating behavior with $\rho_{300K} > 2 \times 10^7$ Ω·cm. The corresponding dielectric permittivity $\varepsilon'$ as a function of temperature curve, recorded during warming (1 K/min), is given in Figure 3a together with the magnetic susceptibility [$\chi(T)$]. It reveals the existence of a clear dielectric anomaly at $T_N$ with a

(31) Engelsman, F. M. R.; Wiegers, G. A.; Jellinek, F.; Van Laar, B. *J. Solid State Chem.* **1973**, *6*, 574.
(32) Le Nagard, N.; Collin, G.; Gorochov, O. *Mater. Res. Bull.* **1979**, *14*, 1411.
(33) Wintenberger, M.; Allain, Y *Solid State Commun.* **1987**, *64*, 1343.
(34) Kawaji, T.; Atake; Saito, Y. *J. Phys. Chem. Solids* **1989**, *50*, 215.
(35) Whittingham, M. S. *Prog. Solid State Chem.* **1978**, *12*, 41.
(36) Hahn, H.; de Lorent, C. *Z. Anorg. Allg. Chem.* **1957**, *290*, 72.
(37) Fullprof software: http://journals.iucr.org/iucr-top/comm/cpd/Newsletters/ or http://www.ill.fr/pages/science/IGroups/diff/Soft/fp/.
(38) Maignan, A.; Martin, C.; Frésard, R.; Eyert, V.; Guilmeau, E.; Hébert, S.; Poienar, M.; Pelloquin, D. *Solid State Commun.* **2009**, *149*, 962.

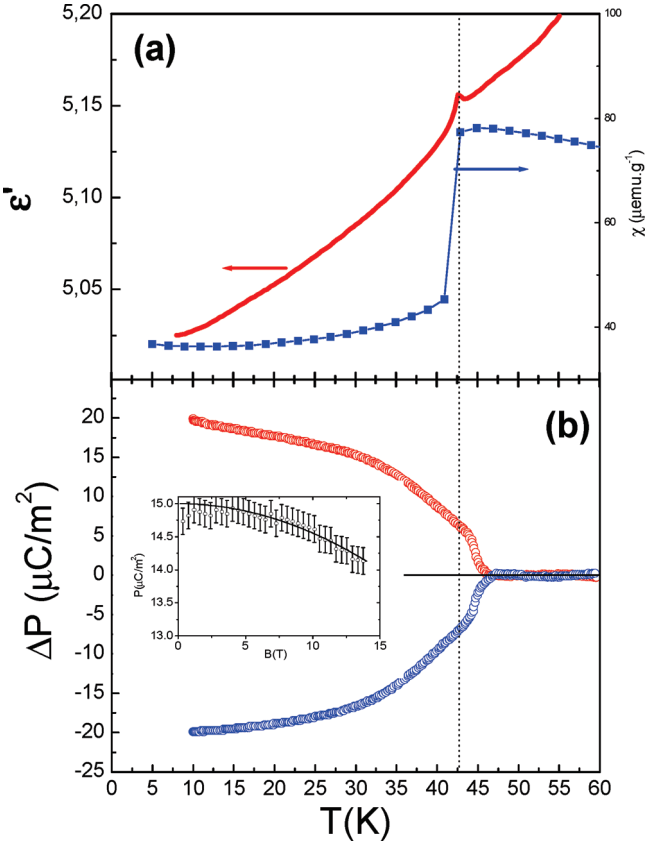


**Figure 3.** (a) $T$ dependence of the dielectric permittivity $\varepsilon'$ (100 kHz, left $y$-axis) and magnetic susceptibility $\chi$ (right $y$-axis) for $AgCrS_2$. The $\varepsilon'$ peak temperature appearing at $T_N$ proves a charge/spin coupling in the insulating $AgCrS_2$ phase. (b) $T$-dependent electrical polarization $P$ ($E$ = 500 kV/m). As $T$ increases, first $\Delta P$ slightly decreases, and second, a clear transition is observed in the $T_N$ region (and $\varepsilon'$ peak). Furthermore, reversing $E$ induces a sign change of $\Delta P$. These results point toward the spin driven ferroelectricity of $AgCrS_2$ which is confirmed by the $P(H)_{T=30K}$ curve given in the inset of part b.

frequency independent peak temperature, confirming the spin/charge coupling. An anomaly is also observed in the imaginary part of the dielectric constant, tan $\delta$ (not shown), with small enough tan $\delta$ values ensuring the relevance of the measurements. The similarity of the magnitude of the $\varepsilon'$ maximum at $T_N$ for $AgCrS_2$ and the magnetoelectrics $ACrO_2$ (A = Ag, Cu)[18] motivated measurements of the electric polarization ($P$) to be made.

The $\Delta P(T)$ curve recorded upon warming at 5 K/min (Figure 3b) shows that the remnant polarization exhibits a maximum value, $\Delta P_{(T=10K)} = 20\,\mu C/m^2$, similar to that found in the $AgCrO_2$ delafossite,[18] and also we observe that $\Delta P$ vanishes at $T_N$. Furthermore, reversing the poling field leads to a symmetric negative polarization as also shown in Figure 3b. This demonstrates that $AgCrS_2$ belongs to the class of the spin induced ferroelectrics. The magnetoelectric coupling can also be observed below $T_N$ on the $P(H)$ curves ($H$ = magnetic field) as shown for $T$ = 30 K in the inset of Figure 3b. A clear $P$ decrease as $H$ increases is observed (Figure 3b) evidencing the existence of magnetoelectric coupling in the antiferromagnetic state.

These results for $AgCrS_2$ emphasize that spin driven ferroelectrics can be discovered in triangular antiferromagnetic chalcogenides providing that they are insulators. Concerning that electronic property, one advantage of $AgCrS_2$ over the $CdCr_2S_4$ spinel[39] results from the more insulating state of the former which prevents possible complications about the exact origin of the colossal magnetocapacitance of the latter.[40] The topology of the magnetic network of $AgCrS_2$ reinforces the importance of the triangular array of magnetic transition metals for searching spin driven ferroelectrics. The property similarities of these sulfides and oxides are also challenging Arima's microscopic model developed for the spin driven ferroelectricity of $CuFeO_2$.[28] As in this framework the necessary ingredients are the p−d orbital hybridization and the spin−orbit coupling, it is remarkable that despite the different natures of the ligands, the properties are similar. It must be emphasized that the $AgCrS_2$ and $AgCrO_2$ crystallographic structures differ: $R3m$ and $R\bar{3}m$, respectively, that is, acentric and centrosymmetric space groups. In that respect, the noncentrosymmetric structure of $AgCrS_2$ is more compatible with the existence of ferroelectricity. Second, though the $AgCrS_2$ and $AgCrO_2$ structures, described as $CrX_6$ layers intercalated with Ag sheets along $c$, are close to each other, the coordination polyhedra are different: (i) regular $CrO_6$ octahedra against $CrS_6$ asymmetric trigonal prisms and (ii) dumbbell O−Ag−O configuration against distorted $AgS_4$ tetrahedra, with three short and one long Ag−S distances. Such structural changes imply differences in the cation−anion−cation orbital hybrization and thus in the magnetic exchanges. Considering the similar ferroelectric behavior found in the $AgCrX_2$ oxide and sulphide that show different p−d orbital hybridizations, it appears thus that this parameter is not the most important one governing the spin driven properties. In contrast, as in both types of compounds, there exists a similar chromium triangular magnetic network, the $Cr^{3+}$−$Cr^{3+}$ direct exchange is most probably playing a major role. In the future, such a new result, obtained by the comparison between oxide and sulphide, will have to be taken into account by the microscopic models.

Finally, the similar multiferroism of $AgCrS_2$ and $AgCrO_2$ strongly suggests that the helimagnetic structure reported for the former[33] is probably also valid for the latter. At this point, neutron powder diffraction is highly needed. Extending the present findings to other $ACrX_2$ compounds, one might also anticipate similar behaviors for isostructural $R3m$ selenides such as $AgCrSe_2$.[31]

**Supporting Information Available:** Details of the sample preparation and the experimental techniques as well as the room temperature X-ray pattern of $AgCrS_2$ with indexation in the $R3m$ space group (the arrow is for the sample holder) (PDF). This material is available free of charge via the Internet at http://pubs.acs.org.

(39) Hemberger, J.; Lunkenheimer, P.; Fichtl, R.; Krug von Nidda, H.-A.; Tsurkan1, V.; Loidl, A. *Nature* **2005**, *434*, 365.
(40) Catalan, G.; Scott, J. F. *Nature* **2007**, *448*, E4.